JCI The Journal of Clinical Investigation

Protein kinase N2 mediates flow-induced eNOS activation and vascular tone regulation

Young-June Jin, Ramesh Chennupati, Rui Li, Guozheng Liang, ShengPeng Wang, András Iring, Johannes Graumann, Nina Wettschureck, Stefan Offermanns

J Clin Invest. 2021. https://doi.org/10.1172/JCI145734.

Research In-Press Preview Cell biology Vascular biology

Graphical abstract

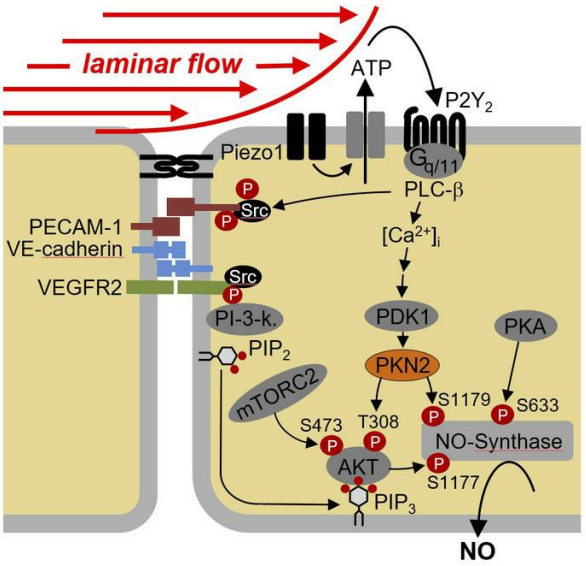

Protein kinase N2 mediates flow-induced eNOS activation and vascular tone regulation

Young-June Jin[1,*], Ramesh Chennupati[1], Rui Li[1], Guozheng Liang[1], ShengPeng Wang[1,2], András Iring[1,3], Johannes Graumann[4], Nina Wettschureck[1,5,6,7], Stefan Offermanns[1,5,6,7,*]

[1] Department of Pharmacology, Max Planck Institute for Heart and Lung Research, Bad Nauheim, Germany.

[2] Cardiovascular Research Center, School of Basic Medical Sciences, Xi'an Jiaotong University Health Science Center, Yanta District, Xi'an, China.

[3] Laboratory of Molecular Medicine, Institute of Experimental Medicine, Hungarian Academy of Sciences Budapest, Hungary.

[4] Scientific Service Group Biomolecular Mass Spectrometry, Max Planck Institute for Heart and Lung Research, Bad Nauheim, Germany.

[5] Centre for Molecular Medicine, Medical Faculty, JW Goethe University Frankfurt, Frankfurt, Germany.

[6] Cardiopulmonary Institute (CPI), Frankfurt, Germany.

[7] German Center for Cardiovascular Research (DZHK), Rhine-Main site, Frankfurt and Bad Nauheim, Germany.

The authors have declared no conflict of interest.

* Corresponding authors: Young-June Jin, Dept. of Pharmacology, Max Planck Institute for Heart and Lung Research, Ludwigstrasse 43, 61231 Bad Nauheim Germany; e-mail: young-june.jin@mpi-bn.mpg.de; phone: +49 6032 705 1268 and Stefan Offermanns, Dept. of Pharmacology, Max Planck Institute for Heart and Lung Research, Ludwigstrasse 43, 61231 Bad Nauheim Germany; e-mail: stefan.offermanns@mpi-bn.mpg.de; phone: +49 6032 705 1201.

Abstract

Formation of nitric oxide (NO) by the endothelial NO-synthase (eNOS) is a central process in the homeostatic regulation of vascular functions including blood pressure regulation and fluid shear stress exerted by the flowing blood is a main stimulus of eNOS activity. Previous work has identified several mechanosensing and -transducing processes in endothelial cells, which mediate this process and result in the stimulation of eNOS activity through phosphorylation of the enzyme via various kinases including AKT. How the initial mechanosensing and signaling processes are linked to eNOS phosphorylation is unclear. In human endothelial cells, we demonstrated that protein kinase N2 (PKN2), which is activated by flow through the mechanosensitive cation channel Piezo1 and G_q/G_{11}-mediated signaling, as well as Ca^{2+} and PDK1, plays a pivotal role in this process. Active PKN2 promoted phosphorylation of human eNOS at serine 1177 and at a newly identified site, serine 1179. These phosphorylation events additively led to increased eNOS activity. PKN2-mediated eNOS phosphorylation at serine 1177 involved phosphorylation of AKT synergistically with mTORC2-mediated AKT phosphorylation while active PKN2 directly phosphorylated human eNOS at serine 1179. Mice with induced endothelium-specific deficiency of PKN2 showed strongly reduced flow-induced vasodilation and developed arterial hypertension accompanied by reduced eNOS activation. These results uncover a central mechanism that couples upstream mechanosignaling processes in endothelial cells to the regulation of eNOS-mediated NO formation, vascular tone and blood pressure.

Introduction

Endothelial cells are located at the interface between the blood and the vessel wall and are centrally involved in autoregulatory processes, which control vascular tone and homeostasis. Nitric oxide (NO) produced by endothelial NO-synthase (eNOS) plays a critical role in these regulatory processes by promoting vascular relaxation and by modulating vascular inflammation and adaptation to physiological and pathophysiological stimuli (1-3). The activity of eNOS is regulated by transcriptional and post-transcriptional mechanisms. Regulation of eNOS activity by fluid shear stress exerted by the flowing blood is one of the major mechanisms controlling basal activity of eNOS. Multiple studies have shown that the eNOS-mediated NO formation in response to sustained flow involves phosphorylation of the enzyme (3-5), and the two best-described residues of human eNOS phosphorylated in response to flow are serine 633 and serine 1177 (4, 6-9). Protein kinase A (PKA) has been reported to be the major enzyme mediating the phosphorylation of serine 633 (8, 10-12), and AKT has been described as the major protein kinase responsible for flow-induced phosphorylation of serine 1177 (6, 7). Later, other related protein kinases, including AMP-activated kinase (AMPK) and PKA have been reported to be also able to mediate flow-induced eNOS phosphorylation at serine 1177 (4, 5, 13, 14).

Flow-induced regulation of AKT-dependent eNOS phosphorylation is mediated by the endothelial mechanosensitive cation channel Piezo1, which is activated by fluid shear stress and promotes release of ATP from endothelial cells which results in the activation of the G_q/G_{11}-coupled purinergic $P2Y_2$ receptor (15). Receptor activation induces downstream signaling processes resulting in the stimulation of AKT activity and the subsequent phosphorylation of human eNOS at serine 1177, which then leads to increased NO formation (16). An important role of AKT1 in flow-induced eNOS phosphorylation and activation has been indicated by knock-down studies *in vitro* (17)

as well as in endothelium-specific Akt1-deficient mice, which show reduced phosphorylation of the corresponding serine residue of mouse eNOS, reduced circulating NO levels and increased blood pressure (18). How the upstream mechanosignaling processes are linked to AKT-dependent eNOS activation is, however, not clear. It has been shown that phosphoinositide-3-kinase (PI-3-kinase) activity plays a role upstream of AKT also in flow-induced endothelial processes (6, 7, 19). However, maximal activation of AKT requires not only binding of the PI-3-kinase product phosphatidylinositol-3,4,5-trisphosphate (PIP_3) to AKT but also phosphorylation of the enzyme at threonine 308 by the phosphoinositide-dependent protein kinase 1 (PDK1) as well as at serine 473 by other kinases such as mTOR complex 2 (mTORC2) or DNA-PK (19, 20). The mechanisms involved in flow-induced phosphorylation and activation of AKT in endothelial cells are still unknown.

Protein kinases N (PKN) are serine/threonine kinases formerly known as protein kinase C-related kinases (PRKs), which consist of the three isoforms PKN1, PKN2 and PKN3 (21, 22). PKN2 shares with the other isoforms an N-terminal antiparallel coiled-coil structure (HR1 domain) that binds to and is activated by Rho family GTPases (23-25) and a C-terminal kinase domain that can be phosphorylated by phosphoinositide-dependent protein kinase 1 (PDK1) promoting PKN activation (26, 27). *In vitro* studies in various cell types have involved PKN2 in the regulation of different cellular functions including cytoskeletal organization, cell migration as well as cell differentiation (28-32). Loss of PKN2 in mice results in morphogenetic and cardiovascular defects and is lethal at embryonic day 10.5 (33, 34).

Here we show that PKN2 plays a central role in flow-induced eNOS regulation by mediating phosphorylation of eNOS at serine 1177 via Akt and by direct phosphorylation of eNOS at serine 1179.

Results

Flow induces phosphorylation of human eNOS at serine 1177 and 1179

In a mass spectrometry-based phosphoproteomic analysis of bovine aortic endothelial cells (BAECs), we found that eNOS is phosphorylated in response to laminar flow not only at serine 635 and 1179, which corresponds to human eNOS serine 633 and 1177, but also at serine 1181, which corresponds to human eNOS serine 1179 (Fig. 1A and B). Increased phosphorylation of bovine and human eNOS at serine 1181 and 1179, respectively, could be validated in BAECs and human umbilical arterial endothelial cells (HUAECs) using a phospho-site-specific antibody (Fig. 1C and D). This antibody specifically recognized a phosphomimetic mutant of human eNOS in which serine 1179 was replaced by aspartic acid (S1179D), while a phosphomimetic mutant of serine 1177 of eNOS (S1177D) was specifically recognized by the anti-phospho serine 1177 antibody (Fig. 1E). Serine residue 1179 of human eNOS and the surrounding sequence are highly conserved in other species (Fig. 1A). Expression of the S1179D mutant of human eNOS resulted, similar to the S1177D mutant, in increased NO formation when expressed in endothelial cells after knockdown of endogenous eNOS (Fig. 1F and Suppl. Fig. 1). A phosphomimetic serine 1177 and 1179 double mutant (S1177D/S1179D) induced a significantly higher increase in NO formation than each of the single mutants (Fig. 1F). This additive effect indicates that both phosphorylation events act independently of each other. After knock-down of endogenous eNOS in HUAECs, re-expression of human eNOS mutants which cannot be phosphorylated anymore (S1177A and S1179A) only partially rescued flow-induced NO formation compared to cells in which wild-type eNOS was re-expressed, and a S1177A/S1179A double mutant showed a further reduced ability to rescue flow-induced NO formation (Fig. 1G). Similarly, carotid arteries from $eNOS^{-/-}$ mice, in which the S1177A and S1179A mutants of eNOS were re-expressed by AAV2-QuadYF-mediated

transduction only partially rescued flow-induced vasorelaxation compared to vessels which expressed wild-type eNOS (Fig. 1H). This indicates that, in addition to phosphorylation of serine 1177, human eNOS is also phosphorylated at serine 1179 in response to flow and that serine 1179 phosphorylation contributes to the flow-induced increase in eNOS activity. Flow-induced eNOS phosphorylation at serine 1179 was not affected by knock-down of AKT1, the major isoform of AKT expressed in endothelial cells, whereas AKT1 knock-down strongly inhibited flow-induced eNOS phosphorylation at serine 1177 (Fig. 1I). Thus, flow-induced phosphorylation of human eNOS at serine 1179 occurs in an AKT-independent manner.

PKN2 is activated by flow and mediates phosphorylation of eNOS at serine 1177 and 1179

In an attempt to identify protein kinases involved in flow-induced eNOS phosphorylation at serine 1179, we performed an siRNA-mediated knock-down of 25 protein kinases highly expressed in human umbilical arterial endothelial cells (HUAECs) and determined the effect on flow-induced phosphorylation of eNOS at serine 1177 and 1179 (Fig. 2A and Suppl. Fig. 2A). Among the kinases whose knock-down significantly reduced flow-induced eNOS phosphorylation at serine 1179 was PKN2 (Fig. 2A). An alternative siRNA directed against PKN2 blocked flow-induced eNOS phosphorylation at serine 1179 and at serine 1177 (Fig. 2B) as well as flow-induced increases in NO levels in cellular supernatants as determined by measurement of nitrite/nitrate levels in HUAECs (Fig. 2C). Corresponding effects were seen after PKN2 knock-down in BAECs (Fig. 2D and E). PKN2 is the major PKN isoform expressed in different endothelial cells followed by PKN1, whereas PKN3 showed lower endothelial expression (Suppl. Fig. 3A). Knock-down of PKN1 expression had no effect on flow-induced eNOS phosphorylation and NO formation in HUAECs (Suppl. Fig. 3C-D).

To test whether PKN2 is activated by laminar flow in endothelial cells, we determined the effect of laminar shear stress on PKN2 kinase activity. Laminar flow increased PKN2 kinase activity as shown by an *in vitro*-kinase assay on immunoprecipitated PKN2 using myelin basic protein (MBP) as substrate (Fig. 2F). Within 5 minutes of applying laminar flow to endothelial cells, we found phosphorylation of PKN2 at threonine 816, which has been shown to result in PKN2 activation (27) (Fig. 2G). Phosphorylation of PKN2 required high shear rates of at least 10 dynes/cm^2 and lasted for at least 24 hours (Fig. 2H and I).

Flow-induced PKN2 activation involves Piezo1, G_q/G_{11} and PDK1 but not PI-3-kinase

RhoA, a known regulator of PKN2 was not involved in flow-induced PKN2 activation as knock-down of RhoA did not affect flow-induced PKN2 phosphorylation (Suppl. Fig. 4A). Since PDK1 has been shown to phosphorylate and thereby activate PKN2 (26, 27, 35) and since knockdown of PDK1 inhibited flow-induced phosphorylation of human eNOS at serine 1179 to a comparable degree as knockdown of PKN2 (Fig. 2A), we tested its involvement in flow-induced PKN2 activation. Knock-down of PDK1 in fact blocked flow-induced PKN2 phosphorylation as well as phosphorylation of eNOS at serine 1177 and 1179 (Fig. 3A). The PDK1 activator PS48 induced a strong phosphorylation of PKN2 as well as of serine 1177 and 1179 of eNOS (Fig. 3B and C), and knock-down of PKN2 inhibited PS48-induced eNOS phosphorylation at serine 1177 and 1179 (Fig. 3C). Similarly, also NO formation induced by PS48 was strongly inhibited by knock-down of PKN2 (Fig. 3D). This indicates that flow-induced PKN2 activation resulting in eNOS phosphorylation is mediated by PDK1.

To understand the upstream regulation of PDK1 and PKN2 in flow-induced signaling, we tested the effect of knock-down or inhibition of known upstream mediators of flow-induced eNOS activation on flow-induced phosphorylation of PKN2.

Knock-down of Piezo1 inhibited phosphorylation of both, PDK1 and PKN2 as well as eNOS phosphorylation at serine 1177 and at serine 1179 (Fig. 3E), and the Piezo1 activator Yoda1 induced phosphorylation of PDK1 and PKN2 (Fig. 3F). The effect of Piezo1 activation on PKN2 phosphorylation was blocked after suppression of PDK1 expression (Fig. 3G). Flow induced activation of Piezo1 resulting in eNOS activation has been shown to involve release of ATP, activation of the endothelial $P2Y_2$ receptor and subsequent G_q/G_{11}-mediated signaling (15, 16). Knock-down of $P2Y_2$ expression with a specific siRNA or pharmacological inhibition of G_q/G_{11} by YM-254890 (36) inhibited flow-induced phosphorylation of both, PDK1 and PKN2 (Fig. 3H and I). Thus, flow-induced activation of PDK1 and PKN2 involves Piezo1 and $P2Y_2/G_q/G_{11}$-mediated signaling.

Piezo1 and G_q/G_{11}-mediated signaling have been shown to mediate flow-induced activation of the mechanosignaling complex consisting of PECAM-1, VE-cadherin and VEGFR2 as well as PI-3-kinase and AKT (15, 16). We therefore tested the effect of inhibition of VEGFR2 by Ki8751 and of PI-3-kinase by wortmannin or LY294002 as well as the effect of an AKT1 knockdown on flow-induced phosphorylation of PDK1, PKN2 and eNOS. Inhibition of VEGFR2 and PI-3-kinase had no effect on flow-induced PDK1 and PKN2 phosphorylation whereas it blocked flow-induced phosphorylation of eNOS at serine 1177 but not phosphorylation of eNOS at serine 1179 (Fig. 4A). Similar to inhibition of VEGFR2, and PI-3-kinase, knock-down of AKT1 did not affect PKN2 phosphorylation in response to flow (Fig. 4B). This indicated that the mechanosignaling complex and PI-3-kinase/AKT are not involved in flow induced activation of PDK1 and PKN2 downstream of Piezo1 and G_q/G_{11}.

We then tested whether the increase in $[Ca^{2+}]_i$ induced by flow through Piezo1 and G_q/G_{11}-mediated signaling (16) is involved in flow-induced activation of PDK1 and PKN2. In fact, chelation of intracellular Ca^{2+} by BAPTA blocked flow-induced phosphorylation of PDK1 and PKN2 (Fig. 4C), and, in addition to the Piezo1 activator

Yoda1, also the Ca^{2+} ionophore ionomycin induced phosphorylation of PDK1 and PKN2 (Fig. 4D). Phosphorylation of PKN2 in response to ionomycin was blocked after suppression of PDK1 expression (Fig. 4E). These data indicate that flow-induced PKN2 phosphorylation is mediated by PDK1 in a manner depending on Piezo1, ATP/$P2Y_2$, G_q/G_{11} and Ca^{2+} but independently of PI-3-kinase (Fig. 4F).

PKN2 mediates eNOS activation by AKT-dependent phosphorylation of serine 1177 and direct phosphorylation of serine 1179

Although activation of PDK1 and PKN2 appears to occur independently of flow-induced activation of the mechanosignaling complex and PI-3-kinase, which have been shown to be required for flow-induced phosphorylation of eNOS at serine 1177 by AKT (16, 37), knock-down of PKN2 and PDK1 blocked flow-induced eNOS phosphorylation at serine 1177 (Figs. 2B and 3A). We therefore tested whether AKT activation by flow requires PKN2 and PDK1. As shown in Fig. 5A and B, knock-down of PKN2 and of PDK1 had no effect on flow-induced AKT phosphorylation at serine 473 but strongly inhibited AKT phosphorylation at threonine 308. Flow-induced AKT phosphorylation at serine 473 was instead blocked by knock-down of the mTORC2 component Rictor (Fig. 5C). Thus, PDK1 and PKN2 act upstream of AKT by mediating phosphorylation at threonine 308 but not of serine 473, which is phosphorylated via mTORC2. Consistent with this, the PDK1 activator PS48 induced AKT phosphorylation at threonine 308 but not at serine 473, and this effect was blocked after knockdown of PKN2 (Fig. 5D). In addition, expression of a constitutively active mutant of PKN2 induced phosphorylation of eNOS both at serine 1177 and serine 1179, however, only phosphorylation at serine 1177 was strongly inhibited after knockdown of AKT1 (Fig. 5E). Similarly, the increased NO production induced by expression of constitutively active PKN2 was partially reduced by knock-down of AKT1 as well as by overexpression of the AKT1 phospho-site mutant T308A (Fig. 5F and G). These data indicate that PKN2 is involved in flow-

induced AKT phosphorylation at threonine 308 and that AKT mediates the PKN2-induced eNOS activation at serine 1177.

As expected from the initial observation that flow-induced phosphorylation of human eNOS at serine 1179 does not involve AKT (Fig. 1H), AKT1 knock-down had no effect on eNOS phosphorylation at serine 1179 induced by active PKN2 but inhibited PKN2-induced eNOS phosphorylation at serine 1177 (Fig. 5E). To test whether PKN2 can directly phosphorylate eNOS at serine 1179, we first tested whether PKN2 and eNOS physically interact. When PKN2 was precipitated from endothelial cells under static conditions, no signal could be detected with an anti-eNOS-antibody in the precipitate. However, after 15 minutes of laminar flow, a relatively strong eNOS signal was seen in the PKN2 precipitate (Fig. 6A). When recombinant eNOS was incubated together with purified PKN2 in the presence of ATP, strong phosphorylation of serine 1179 but not of serine 1177 was observed (Fig. 6B and C). These data indicate that PKN2 can interact with eNOS and phosphorylate serine 1179 of eNOS, suggesting that PKN2 induces eNOS activation in response to flow through AKT-dependent phosphorylation of serine 1177 as well as by direct phosphorylation of eNOS at serine 1179 (Fig. 6D).

Endothelial PKN2 deficiency results in hypertension and loss of flow-induced vasodilation

To test whether PKN2-mediated endothelial eNOS activation is physiologically relevant, we generated mice with tamoxifen-inducible endothelium-specific PKN2 deficiency (Tek-CreER^{T2};Pkn2$^{fl/fl}$, herein referred to as EC-Pkn2-KO) (Fig. 7A). Precontracted aortic segments from induced EC-Pkn2-KO mice showed normal relaxation in response to acetylcholine (Fig. 7B). However, endothelial loss of PKN2 resulted in a strong reduction of flow-induced dilation of precontracted mesenteric vessels (Fig. 7C). We then tested the effect of an acute induction of endothelial Pkn2

deficiency on telemetrically recorded blood pressure in conscious mice. Treatment of wild-type mice with tamoxifen resulted in a transient increase in arterial blood pressure (Fig. 7D). However, induction of endothelial Pkn2 deficiency led to a sustained increase in arterial blood pressure by 20 mmHg. A very similar increase in blood pressure was seen after induction of Cdh5-CreERT2;Pkn2$^{flox/flox}$ mice (Suppl. Fig. 5A and B). Induction of endothelial Pkn1 deficiency had no effect on the blood pressure (Fig. 7D) consistent with a lack of any effect of Pkn1 knock-down on flow-induced eNOS activation *in vitro*. In parallel to the increase in arterial blood pressure after induction of endothelium-specific Pkn2 deficiency, we observed a reduced phosphorylation of murine mesenteric artery eNOS at serine 1176 and serine 1178, corresponding to serine 1177 and serine 1179 in human eNOS, respectively (Fig. 7E). The reduced phosphorylation of eNOS in mice with induced endothelial PKN2 deficiency was accompanied by a decrease in plasma nitrite/nitrate levels (Fig. 7F). These data indicate that the acute loss of PKN2-mediated signaling in the endothelium results in reduced eNOS activity, leading to increased vascular tone and blood pressure.

Discussion

The regulation of eNOS is a complex process involving different upstream stimuli and several mechanisms including posttranslational modifications (3, 4, 9). Fluid shear stress exerted by the flowing blood is one of the most important stimuli of eNOS activity which is centrally involved in basal control of vascular functions such as vascular tone and blood pressure. In the past, two major pathways were described to regulate eNOS activity in response to fluid shear stress. One is initiated by flow-induced release of adrenomedullin and subsequent activation of cAMP formation and protein kinase A through the adrenomedullin receptor resulting in phosphorylation of human eNOS at serine 633 (4, 8, 9, 12, 38). The other one is initiated by the release of ATP, which, through activation of $P2Y_2$ receptors and the G_q/G_{11}-mediated signaling pathway, results in activation of AKT and phosphorylation of human eNOS at serine 1177 (3, 4, 6, 7, 16). Upstream regulation of both pathways has been shown to involve activation of the mechanosensitive cation channel Piezo1 (12, 15). While previous research had shown that flow-induced G_q/G_{11}-mediated activation of AKT involves a mechanosignaling complex including VEGFR2 (16, 37), the direct mechanism of flow-induced AKT activation has remained unclear. Here we show that AKT activation and subsequent eNOS phosphorylation at serine 1177 in response to flow required PKN2 and that PKN2 in addition also leads to phosphorylation of eNOS at serine 1179. We also demonstrate that these effects are additive and we identified the upstream regulation of flow-induced PKN2 activation, which involved $P2Y_2$- and G_q/G_{11}-mediated increases in intracellular Ca^{2+} and subsequent PDK1 activation (Fig. 6D). The fact that acute loss of endothelial PKN2 leads to reduced eNOS activity, reduced flow-induced vasodilation and to hypertension *in vivo* indicates that this ~~new~~ PKN2-mediated signaling pathway in endothelial cells is constantly activated to mediate fluid shear stress-induced endothelial NO formation and vasodilation.

The central role of AKT in eNOS phosphorylation and activation is well established (6, 7, 39), and viral transduction of a constitutively active AKT resulted in increased NO release and enhanced blood flow *in vivo* (40). Similar results were observed after endothelial cell-specific expression of an active version of AKT, which resulted in increased NO production (41). That AKT-mediated regulation of eNOS activity *in vivo* is mediated by phosphorylation of eNOS at serine 1177 was further supported by the observation that the corresponding phosphomimetic murine eNOS mutant S1176D can rescue the vascular phenotype observed in AKT1-deficient mice (39) as well as by the finding that endothelial cell-specific AKT1-deficient mice have reduced plasma NO levels, reduced phosphorylation of murine eNOS at serine 1176 in blood vessels as well as increased blood pressure (18). The mechanism by which AKT is activated by fluid shear stress has however remained unclear. A general requirement for AKT activation is the stimulation of phosphoinositide-3-kinase (PI-3-K), leading to PtdIns-3,4,5-P_3 (PIP_3) formation which recruits AKT to the membrane through interaction with its PH domain (19, 20, 42). Consistent with this, fluid shear stress has been shown to induce activation of PI-3-kinase (37, 43). However, full activation of the AKT kinase activity requires phosphorylation of AKT at threonine 308 in the catalytic domain of the kinase, which typically involves PDK1 (19, 20, 44, 45) as well as phosphorylation of serine 473 in a C-terminal hydrophobic motif mainly mediated by mTORC2 (46, 47). Whether flow-induced endothelial AKT activation also involved PDK1- and mTORC2-mediated phosphorylation was however unknown. Our data clearly show that disruption of mTORC2 by suppression of Rictor expression blocked flow-induced AKT phosphorylation at serine 473, but not at threonine 308. Flow-induced AKT phosphorylation at threonine 308 was blocked after knock-down of PDK1 and also of PKN2, whereas in both cases phosphorylation of serine 473 was unaffected. The specific phosphorylation of AKT at threonine 308 could be mimicked by the PDK1 activator PS48, which also induced a strong phosphorylation of PKN2. Interestingly,

the effect of PS48 on AKT phosphorylation at threonine 308 was blocked after knock-down of PKN2. This indicated that flow-induced AKT phosphorylation at threonine 308 through PDK1 does not occur directly, but is mediated by PKN2 in endothelial cells exposed to flow. This function of PKN2 to mediate PDK1-induced phosphorylation of AKT at threonine 308 is consistent with several *in vitro* reports showing that PKN2 is a substrate of PDK1 and can be activated through PDK1-mediated phosphorylation (26, 27, 35). In addition, there is also evidence that PKN2 and AKT1 interact (48, 49) and that PKN2 can activate AKT (32). We conclude that flow-induced activation of endothelial AKT involves PI-3-kinase/mTORC2-mediated phosphorylation at serine 473 and phosphorylation at threonine 308 through an atypical mechanism involving PKN2 which is activated by PDK1 (Fig. 6D).

PKNs have been described to be activated by binding to members of the Rho family of GTPases through a Rho-binding motif known as the HR1 domain (23-25). However, we did not find any evidence for a role of Rho-GTPases in flow-induced endothelial PKN2 activation. This is consistent with published data that RhoA is not activated in response to acute flow in endothelial cells (50). We rather found that flow-induced PKN2 activation in endothelial cells is mediated by PDK1. Interestingly, this PDK1-mediated PKN2 activation was independent of PI-3-kinase and VEGFR2, as their inhibition did not affect flow-induced phosphorylation of PKN2 and PDK1 while inhibition of PI-3-kinase and VEGFR2 blocked flow-induced AKT phosphorylation at serine 473 (16, 51). This indicates that flow-induced activation of PDK1/PKN2 occurs independently of the mechanosignaling complex consisting of PECAM-1, VE-cadherin and VEGFR2, which mediates flow-induced activation of PI-3-kinase (37). Instead we found that flow-induced activation of PKN2 was blocked after knock-down of Piezo1 and $P2Y_2$, inhibition of G_q/G_{11} and chelation of intracellular Ca^{2+} using BAPTA, while it could be induced by the Piezo1 activator Yoda1 and by the calcium ionophore ionomycin. This strongly indicates that flow-induced activation of PDK1/PKN2 is a

calcium-mediated process downstream of Piezo1 and G_q/G_{11} (Fig. 6D). This is consistent with earlier data showing that Ca^{2+} can activate PDK1 (52) and that Ca^{2+}-induced phosphorylation of Akt at threonine 308 involves PDK1 (53).

Serine 1177 is one of the most extensively studied phosphorylation sites of human eNOS and several *in vitro* studies have shown that a phospho-mimetic mutant, in which serine 1177 is replaced by aspartic acid (S1177D), has an increased basal activity (6, 7). Conversely, endothelial cells expressing the phosphosite mutant S1177A show reduced flow-induced NO formation (12). Knock-in mice expressing the corresponding phosphomimetic S1176D mutant of mouse eNOS show increased endothelium-dependent vasodilation, whereas mice expressing the phosphosite mutant S1176A have reduced endothelium-dependent vasodilation and an increase in blood pressure (54-56). While this represents strong evidence for a role of serine 1177 phosphorylation in the regulation of human eNOS activity *in vitro* and *in vivo*, a recent *in vitro* study has challenged this view and found that eNOS phosphorylation at serine 1177 does not correlate with increased activity of the enzyme (57). The reason for this discrepancy is still unclear, but flow-induced effects were not analyzed in this study. Mechanistically it has been suggested that the C-terminal region of the enzyme to which serine 1177 is located has an autoinhibitory function and that phosphorylation at serine 1177 reduces this autoinhibition (58-60). Our data show that in addition to serine 1177 also serine 1179 in human eNOS as well as the corresponding serine residue in bovine eNOS is phosphorylated in response to flow. This serine residue is highly conserved in different species, and its phosphorylation might have been overseen in previous analyses. We show that serine 1177 and 1179 are phosphorylated independently of each other by different mechanisms involving the classic PI-3 kinase/mTORC2/AKT pathway as well as a new mechanism mediated by PKN2. Importantly, both phosphorylation events promote eNOS activation in an additive

fashion. Whether the additivity of the effects of both phosphorylations on eNOS activity is due to the same of different mechanisms is currently not clear.

Our results identify serine 1179 of human eNOS as an additional phosphorylation site, which, together with the well-established serine 1177 phosphorylation, additively regulates eNOS activity. Both serine residues are phosphorylated in response to fluid shear stress through different pathways, a PI-3-kinase- and mTORC2-dependent pathway, resulting in AKT phosphorylation at serine 473 to induce serine 1177 phosphorylation of eNOS as well as through an independent pathway involving Ca^{2+}, PKD1 and PKN2, resulting in phosphorylation of serine residue serine 1179 of human eNOS. PKN2 also plays an important role in serine 1177 phosphorylation as it phosphorylates AKT at threonine 308 in response to flow and thereby promotes AKT-dependent serine 1177 phosphorylation of human eNOS. Thus, our data favor a model, in which PKN2 integrates different flow-induced signaling pathways to link them to phosphorylation-dependent eNOS activation. It will be interesting to see whether the PKN2-mediated endothelial signaling process is affected in pathological situations, in which eNOS activity is impaired, and whether PKN2 is also involved in other flow-independent mechanisms of eNOS activity regulation.

Methods

Reagents. Acetylcholine, phenylephrine, sodium nitroprusside (SNP), BAPTA-AM (1,2-Bis (2-aminophenoxy) ethane -N,N,N′,N′- tetraacetic acid tetrakis(acetoxymethyl ester)), PS48, ionomycin, KN93, wortmannin, LY294002, Ki8751 and tamoxifen were purchased from Sigma-Aldrich (St. Louis, MO, USA). YM-254890 was from FUJI FILM Wako Chemicals (cat. no.: 257-00631). Yoda1 was from Maybridge (cat. no.: SPB07298). Antibodies directed against phosphorylated eNOS (mouse S1176, human S1177, and bovine S1179; cat. no.: 9571), phosphorylated AKT (S473; cat. no.: 4060), phosphorylated AKT (T308; cat. no.: 13038), AKT (cat. no.: 9272), phosphorylated PDK1 (S241; cat. no.: 3438), PDK1 (cat. no.: 5662), phosphorylated PKN2 (T816; cat. no.: 2611), PKN2 (cat. no.: 2612), RhoA (cat. no.: 2117), Rictor (cat. no.: 2114), GAPDH (cat. no.: 2118) and Tubulin (cat. no.: 2521S) were obtained from Cell Signaling Technology. Antibody directed against phosphorylated eNOS (mouse S1178, human S1179, and bovine S1181; cat. no.: PA5-64532) was obtained from Thermofisher scientific. Anti-eNOS (cat. no.: 610296) and PKN1 (cat. no.: 610687) antibody were purchased from BD Biosciences). Anti-$P2Y_2$ antibody was from Alomone Labs (cat. no.: APR-010). Anti-PIEZO1 antibody was from Proteintech (cat. no.: 15939-1-AP).

Primary cells. Human umbilical artery endothelial cells (HUAEC) and bovine aortic endothelial cells (BAEC) were purchased from Provitro AG and cultured in EGM-2 MV medium (Lonza, Basel, Switzerland). RFL-6 rat fibroblast cells (CCL-192) were purchased from American Type Culture Collections (ATCC, Manassas, VA, USA) and were cultured in F-12 Nutrient Mixture (Ham, Invitrogen) containing 10% FCS.

siRNA-mediated knockdown. Endothelial Cells were transfected with siRNA using Opti-MEM (Thermo Fisher) and Lipofectamine RNAiMAX (Invitrogen) as described previously (16). siRNAs used for screening were pools of three siRNA directed against non-receptor tyrosine kinase which show high expression in HUAEC and BAECs and were obtained from Sigma-Aldrich. The targeted sequences are shown in Suppl. Tab. 1. Other siRNAs used were against the following sequences: 5-GTGTTTGGTCTCAAGGACT-3 and 5-GTGTCTACTTCCTGCTCTT-3 (PIEZO1), and 5-CCCTTCAGCACGGTGCTCT-3', 5'-CTGCCTAGGGCCAAGCGCA-3 (P2RY2). The PDK1 esiRNA (#EHU079981), Rictor esiRNA (#EHU076781) and control siRNAs (#SIC001) were purchased from Sigma-Aldrich.

Shear stress assays. Endothelial cells were seeded on µ-Slide I Luer (Ibidi, 80176) and laminar flow was applied on confluent monolayers using the Ibidi pump system chamber (ibidi, Germany). The constant wall shear stress (τ) is given by $\tau = \eta \times 131.6 \varphi$; η: viscosity of the medium; φ: flow rate (according to manufacturer's instructions).

Western blotting. Endothelial cells and mesenteric arteries were lysed in RIPA buffer freshly supplemented with protease and phosphatase inhibitors (PhosSTOP™, Roche). Total cell lysates subjected to SDS-PAGE electrophoresis and transferred to PVDF membranes. After blocking with 5% BSA for 1 hour, the membranes were incubated with primary antibodies overnight at 4°C. The membranes were incubated with HRP-conjugated secondary antibodies for 1 hour at RT (Cell Signaling, dilution 1:3,000) followed by chemiluminescence detection using ECL substrate (Pierce) according to the manufacturer's protocol. The intensities of protein bands were quantitated using ImageJ Gel Analysis program (NIH).

***In vitro* kinase and phosphorylation assay.** Kinase activity was determined by performing an *in vitro* kinase assay (61). Briefly, endothelial cells were lysed in RIPA buffer containing protease inhibitors (complete protease inhibitor cocktail, Roche) and phosphatase inhibitors (PhosSTOP^{TM}, Roche), and after centrifugation (30.000 x g, 15 min) the supernatant was incubated with 3 µg of the anti-PKN2 antibody overnight at 4 °C on a rotating platform. Thereafter, 30 µl of protein A/G-Sepharose beads pre-equilibrated in RIPA buffer were added and incubated for 1 hour at 4 °C. A/G-Sepharose beads were then collected by centrifugation at 3.500 x g for 1 min and were washed 3 times and resuspended in washing buffer (20 mM Tris-HCl [pH7.4], 10 mM $MgCl_2$). Pellets were resuspended in 20 µl of kinase buffer (20 mM Hepes, pH 7.4, 10 mM MgAc, 1 mM dithiothreitol, 50 µM ATP, 20 µCi of [γ-^{32}P]-ATP (Hartmann Analytic, Germany), together with 1 µg of MBP (cat.no.: C1416, Santa Cruz Biotechnology Inc.) as substrate for 30 min at room temperature. To stop the reaction, SDS-PAGE loading buffer was added. The reaction mixture was separated by SDS-PAGE and ^{32}P-labeled proteins were visualized by autoradiography. For *in vitro* eNOS phosphorylation by PKN2, purified full-length human eNOS (cat. no.: ALX-201-853-0010, Enzo Life Sciences) and PKN2 (P71-10G-05, SignalChem) were mixed and incubated for 30 min at 30°C with 10 µCi of [γ-^{32}P]-ATP in 20 µl of kinase buffer. All reactions were terminated by adding SDS-PAGE loading buffer. Proteins were separated by SDS-PAGE, and the gels were stained with Coomassie. The radioactivity was analyzed by autoradiography. Alternatively, *in vitro* eNOS phosphorylation by PKN2 was detected by immunoblotting by using the anti-phospho-eNOS S1179 antibody.

Animal models. All mice were backcrossed onto a C57BL/6N background at least 8 to 10 times, and experiments were performed with littermates as controls. Male and female animals (8–12 weeks old) were used unless stated otherwise. Mice were housed under a 12-hour light- dark cycle, with free access to food and water and under

specific pathogen-free conditions unless stated otherwise. The endothelium-specific Cre transgenic lines Tek-CreERT2 and Cdh5-CreERT2 have been described previously (62, 63). Embryonic stem (ES) cells heterozygous for a targeted allele of *Pkn1* or *Pkn2*, which, after removal of a cassette flanked by FRT-sites, allows for Cre-mediated recombination, have been purchased from KOMP repository (The Knockout Mouse Project, Davis, CA 95616 USA). ES cell clones were injected into C57BL/6 blastocysts and were transferred to pseudo-pregnant females. Chimeric offspring were bred with C57BL/6 mice to produce heterozygous animals. The germ line transmission was confirmed in the F1 generation using a PCR genotyping strategy. In order to remove the selection cassette, mice were crossed to Flp-deleter mice (64) and were subsequently crossed with Tek-CreERT2 mice and Cdh5-CreERT2 mice to obtain animals with inducible endothelium-specific deficiency (EC-Pkn1-KO or EC-Pkn2-KO). $eNOS^{-/-}$ mice (B6.129P2-Nos3tm1Unc/1) were obtained from the Jackson Laboratories (Bar Harbor, ME, USA).

Determination of nitrate and nitrite (NOx) and cGMP levels. Nitrate and nitrite (NOx) levels were measured as described previously (12). In brief, blood collected by venous puncture was immediately centrifuged at 6,800 *g* for 5 minutes at 4°C, and 20 µl plasma was used for nitrate measurement. For experiment to determine flow-induced nitrate release from endothelial cells, cells were plated on culture glass of the BioTech-Flow viscometer chambers (MOS Technologies). Cells were starved in serum-free medium for 6 h and were exposed to laminar flow for 30 min. Nitrate and nitrite production was measured based on nitrite and nitrate accumulation in the medium and plasma using a nitrate/nitrite fluorometric assay kit from Cayman Chemical according to the manufacturer's instructions.

Cyclic GMP levels were measured using the RFL-6 reporter cell assay as described (65). RFL-6 cells were grown to confluence in 6-well plates and washed

twice in Locke's solution (154 mM NaCl, 5.6 mM KCl, 2 mM $CaCl_2$, 1 mM $MgCl_2$, and 10 mM HEPES) containing 0.3 mM 3-isobutyl-1-methylxanthine (IBMX) before the experiment. RFL-6 cells were incubated with supernatants of HUAECs expressing control vector, wild-type eNOS or mutants of eNOS in the absence or presence of L-NAME (1 μM). Thereafter, the incubation was stopped by the addition of ice-cold 50 mM sodium acetate buffer (pH 4.0). The cells were then lysed and cyclic GMP concentration was determined using the cGMP assay kit according to the manufacturer's instructions (Abcam, Cambridge, MA, USA, Cat. #ab65356).

Wire myography. Two weeks after the last tamoxifen injection, mice were sacrificed by CO_2 inhalation. Intact first order mesenteric arteries (2 mm) were isolated from the mesentery and mounted on a conventional myograph setup (610-M, Danish Myo Technology) and kept in Krebs solution (118.1 mM NaCl, 4.8 mM KCl, 2.5 mM $CaCl_2$, 1.2 mM $MgSO_4$, 1.2 mM KH_2PO_4, 25 mM $NaHCO_3$, 9.3 mM glucose, and 0.026 mM EDTA). Arterial segments were distended to the diameter at which maximal contractile responses to 10 μM phenylephrine were observed (Dopt) (66). After a 30-min recovery period of normalization, the contractile and relaxation responses to the indicated agonists were tested. All arterial segments were allowed 30 min of recovery after normalization. Endothelial integrity was checked, the segments which show lower than 80% relaxation were excluded from experiment.

Pressure myography. Pressure myograph experiments were performed as described previously (16). In brief, 10-14 days after tamoxifen injection, second order mesenteric arteries were removed from the mesentery and were mounted between 2 glass micropipettes seated in a pressure myograph chamber (Danish Myo Technology; 114P). The temperature of the chamber was kept at a constant 37°C during the experiment. The mounted artery was initially pressurized to 20 mmHg under no-flow

conditions and incubated for 30 minutes. Pressure was then increased to 60 mmHg and the vessel was incubated for 10 minutes to allow it to reach a steady-state diameter. Arterial segments were contracted with 50 to 150 nM U46619 to 40% to 50% of the passive diameter. After reaching a stable baseline, flow was increased in a stepwise manner by changing the pressure of the inflow and outflow sides inversely, thereby creating a pressure difference inside the lumen of artery without altering the intraluminal pressure. The viability of the vessel was verified at the end of the experiment by dilating the vessel with acetylcholine (10 μM). Arteries showing less than 60% relaxation were considered damaged and were omitted from further analysis. Vasodilatation to flow was calculated as a percentage of the U46619-induced contraction as described previously (67) by the following equation: percentage of relaxation = $100 \times (D_F - DU_{46619})/(DP_D - DU_{46619})$, where D represents the external diameter of the vessels; D_F is the vessel diameter during flow; DU_{46619} is the diameter after U46619 contraction; and DP_D is the passive diameter without any treatment.

Telemetric blood pressure measurements. Measurements were performed in conscious, unrestrained mice with a radiotelemetry system (PA-C10; Data Sciences International) as described previously (12). Mice were caged with blinded identity and in random order.

Lentiviral infection of cells. Human wild-type or mutant forms of eNOS, Akt1 and PKN2 were cloned into the lentiviral pLVX-IRES-ZsGreen1 expression vector (Clontech, Mountain View, CA, USA) and were transfected into HEK293T cells along with envelope plasmid pMD2.G and packaging plasmid psPAX2 using Lipofectamine™ 3000 Transfection Reagent (Thermo fisher Scientific) according to the manufacturer's protocol. Following 48 hours, supernatants containing lentiviral particles were harvested and filtered through 0.45 μm low-protein binding durapore membrane

(Millex) to remove cell debris. HUAECs were previously transfected with siRNA against human eNOS or AKT using Opti-MEM and Lipofectamine RNAiMAX (Invitrogen). For lentiviral transduction, HUAECs were seeded in 6-well plates and the concentrated lentivirus was added. After 48 hours, cells were used for further analyses.

AAV infection. Adeno-associated virus 2-QuadYF carrying the cDNA encoding eNOS WT, the S1177A and S1179A mutant of eNOS as well as EGFP were generated by Vectorbuilder (Cyagen Biosciences). 10-12 week-old $eNOS^{-/-}$ mice were anesthetized by isofluorane inhalation. Mice were given AAV2-QuadYF-eNOS WT, S1177A, S1179A or AAV2-QuadYF-EGFP (1×10^{11} viral genomes in 100 µl saline) by intravenous injection. 1 week after virus injection, carotid arteries were harvested to measure gene expression and flow-induced vasorelaxation using a pressure myography system.

Expression analysis. Total RNA was isolated using an RNeasy Micro Kit (Qiagen), according to the manufacturer's instructions. Reverse transcription (RT) was performed using the ProtoScript II Reverse Transcription kit (New England BioLabs, M0368S). The resulting cDNA was used as a template for quantitative PCR (qPCR) reactions using the LightCycler 480 Probe Master System (Roche), following the manufacturer's protocol. The primer sequences are listed in Suppl. Tab. 2. The resulting Cq values were analyzed and normalized to the reference gene *GAPDH.*

Proteomic and phosphoproteomic analysis. Samples were prepared as described earlier (Iring et al., 2019) with modifications. Cells were lyzed in 4% SDS, 100 mM Tris, pH 7.6 without protease inhibitor by 10 min boiling followed by sonication prior to removal of cell debris by centrifugation. Further, samples were labeled using reductive dimethylation as reported (68) and STAGE tipping of proteomic samples omitted. Using

MARMoSET (69), liquid chromatography/tandem mass spectrometry (LC/MS2) instrumentation parameters were extracted as well as summarized from raw data files and are included in the supplemental material. Peptide/spectrum matching and quantitation were performed using the MaxQuant suite of algorithms (70, 71) against the UniProt (72) mouse canonical and isoforms bovine data base (downloaded on 2019/08/19; 46,707 entries) with parameters also included in the supplemental information. Intensity values of the phospho-sites shown were normalized to eNOS intensity and thus protein abundance in the proteome.

Statistics. All statistical analysis was performed using the GraphPad Prism software v.6.07 from GraphPad Software Inc. (La Jolla, CA, USA). All experimental values are presented as means ± s.e.m. Statistical significance was tested using either an ANOVA or unpaired Student's t-tests. Statistical analysis between two groups were performed with an unpaired two-tailed Student's t-test, multiple group comparisons were analyzed with one-way ANOVA followed by Tukey's post-hoc test, and comparisons between multiple experimental group at different time points were performed using two-way ANOVA followed by Bonferroni's post-hoc test. A *p*-value of less than 0.05 was considered to be statistically significant.

Study approval. All procedures involving animal care and use in this study were approved by the local animal ethics committees (Regierungspräsidium Darmstadt, Germany).

Author contributions

Y.J.J. performed most experiments, designed the study, analyzed and discussed data and contributed to writing the manuscript. R.C., R.L., G.L., and S.P.W. helped with myography experiments and blood pressure measurement. A.I. and J.G. performed phosphoproteomic analysis. N.W. supervised the study, discussed data, and commented on the manuscript. S.O. initiated and supervised the study, discussed data and wrote the manuscript. All authors read and commented on the manuscript.

Acknowledgements

We thank Svea Hümmer for secretarial help and Ulrike Krüger, Claudia Ullmann, Martina Finkbeiner, and Sylvia Jeratsch for expert technical support. This work was supported by the Collaborative Research Center 834 of the German Research Foundation, the Hungarian Academy of Sciences Premium Postdoctoral Research Program (PPD2019-20/2019-439 to A.I.) and a fellowship to Y.J.J. of the Alexander von Humboldt Foundation.

References

1. Zhao Y, Vanhoutte PM, and Leung SW. Vascular nitric oxide: Beyond eNOS. *J Pharmacol Sci.* 2015;129(2):83-94.

2. Siragusa M, and Fleming I. The eNOS signalosome and its link to endothelial dysfunction. *Pflugers Arch.* 2016;468(7):1125-37.

3. Garcia V, and Sessa WC. Endothelial NOS: perspective and recent developments. *Br J Pharmacol.* 2019;176(2):189-96.

4. Fleming I. Molecular mechanisms underlying the activation of eNOS. *Pflugers Arch.* 2010;459(6):793-806.

5. Balligand JL, Feron O, and Dessy C. eNOS activation by physical forces: from short-term regulation of contraction to chronic remodeling of cardiovascular tissues. *Physiol Rev.* 2009;89(2):481-534.

6. Fulton D, Gratton JP, McCabe TJ, Fontana J, Fujio Y, Walsh K, et al. Regulation of endothelium-derived nitric oxide production by the protein kinase Akt. *Nature.* 1999;399(6736):597-601.

7. Dimmeler S, Fleming I, Fisslthaler B, Hermann C, Busse R, and Zeiher AM. Activation of nitric oxide synthase in endothelial cells by Akt-dependent phosphorylation. *Nature.* 1999;399(6736):601-5.

8. Boo YC, Hwang J, Sykes M, Michell BJ, Kemp BE, Lum H, et al. Shear stress stimulates phosphorylation of eNOS at Ser(635) by a protein kinase A-dependent mechanism. *Am J Physiol Heart Circ Physiol.* 2002;283(5):H1819-28.

9. Qian J, and Fulton D. Post-translational regulation of endothelial nitric oxide synthase in vascular endothelium. *Front Physiol.* 2013;4:347.

10. Bauer PM, Fulton D, Boo YC, Sorescu GP, Kemp BE, Jo H, et al. Compensatory phosphorylation and protein-protein interactions revealed by loss of function and gain of function mutants of multiple serine phosphorylation sites in endothelial nitric-oxide synthase. *J Biol Chem.* 2003;278(17):14841-9.

11. Michell BJ, Harris MB, Chen ZP, Ju H, Venema VJ, Blackstone MA, et al. Identification of regulatory sites of phosphorylation of the bovine endothelial nitric-oxide synthase at serine 617 and serine 635. *J Biol Chem.* 2002;277(44):42344-51.

12. Iring A, Jin YJ, Albarran-Juarez J, Siragusa M, Wang S, Dancs PT, et al. Shear stress-induced endothelial adrenomedullin signaling regulates vascular tone and blood pressure. *J Clin Invest.* 2019;130:2775-91.

13. Boo YC, Sorescu G, Boyd N, Shiojima I, Walsh K, Du J, et al. Shear stress stimulates phosphorylation of endothelial nitric-oxide synthase at Ser1179 by Akt-independent mechanisms: role of protein kinase A. *J Biol Chem.* 2002;277(5):3388-96.

14. Zhang Y, Lee TS, Kolb EM, Sun K, Lu X, Sladek FM, et al. AMP-activated protein kinase is involved in endothelial NO synthase activation in response to shear stress. *Arterioscler Thromb Vasc Biol.* 2006;26(6):1281-7.

15. Wang S, Chennupati R, Kaur H, Iring A, Wettschureck N, and Offermanns S. Endothelial cation channel PIEZO1 controls blood pressure by mediating flow-induced ATP release. *J Clin Invest.* 2016;126(12):4527-36.

16. Wang S, Iring A, Strilic B, Albarrán Juárez J, Kaur H, Troidl K, et al. $P2Y_2$ and Gq/G_{11} control blood pressure by mediating endothelial mechanotransduction. *J Clin Invest.* 2015;125(8):3077-86.

17. Koo A, Nordsletten D, Umeton R, Yankama B, Ayyadurai S, Garcia-Cardena G, et al. In silico modeling of shear-stress-induced nitric oxide production in endothelial cells through systems biology. *Biophys J.* 2013;104(10):2295-306.

18. Lee MY, Gamez-Mendez A, Zhang J, Zhuang Z, Vinyard DJ, Kraehling J, et al. Endothelial Cell Autonomous Role of Akt1: Regulation of Vascular Tone and Ischemia-Induced Arteriogenesis. *Arterioscler Thromb Vasc Biol.* 2018;38(4):870-9.

19. Manning BD, and Toker A. AKT/PKB Signaling: Navigating the Network. *Cell.* 2017;169(3):381-405.

20. Hers I, Vincent EE, and Tavare JM. Akt signalling in health and disease. *Cell Signal.* 2011;23(10):1515-27.

21. Marrocco V, Bogomolovas J, Ehler E, Dos Remedios CG, Yu J, Gao C, et al. PKC and PKN in heart disease. *J Mol Cell Cardiol.* 2019;128:212-26.

22. Thumkeo D, Watanabe S, and Narumiya S. Physiological roles of Rho and Rho effectors in mammals. *Eur J Cell Biol.* 2013;92(10-11):303-15.

23. Watanabe G, Saito Y, Madaule P, Ishizaki T, Fujisawa K, Morii N, et al. Protein kinase N (PKN) and PKN-related protein rhophilin as targets of small GTPase Rho. *Science.* 1996;271(5249):645-8.

24. Hutchinson CL, Lowe PN, McLaughlin SH, Mott HR, and Owen D. Differential binding of RhoA, RhoB, and RhoC to protein kinase C-related kinase (PRK) isoforms PRK1, PRK2, and PRK3: PRKs have the highest affinity for RhoB. *Biochemistry.* 2013;52(45):7999-8011.

25. Amano M, Mukai H, Ono Y, Chihara K, Matsui T, Hamajima Y, et al. Identification of a putative target for Rho as the serine-threonine kinase protein kinase N. *Science.* 1996;271(5249):648-50.

26. Dettori R, Sonzogni S, Meyer L, Lopez-Garcia LA, Morrice NA, Zeuzem S, et al. Regulation of the interaction between protein kinase C-related protein kinase 2 (PRK2) and its upstream kinase, 3-phosphoinositide-dependent protein kinase 1 (PDK1). *J Biol Chem.* 2009;284(44):30318-27.

27. Balendran A, Biondi RM, Cheung PC, Casamayor A, Deak M, and Alessi DR. A 3-phosphoinositide-dependent protein kinase-1 (PDK1) docking site is required for the phosphorylation of protein kinase Czeta (PKCzeta) and PKC-related kinase 2 by PDK1. *J Biol Chem.* 2000;275(27):20806-13.

28. Vincent S, and Settleman J. The PRK2 kinase is a potential effector target of both Rho and Rac GTPases and regulates actin cytoskeletal organization. *Mol Cell Biol.* 1997;17(4):2247-56.

29. Lachmann S, Jevons A, De Rycker M, Casamassima A, Radtke S, Collazos A, et al. Regulatory domain selectivity in the cell-type specific PKN-dependence of cell migration. *PLoS One.* 2011;6(7):e21732.

30. Bourguignon LY, Singleton PA, and Diedrich F. Hyaluronan-CD44 interaction with Rac1-dependent protein kinase N-gamma promotes phospholipase Cgamma1 activation, Ca(2+) signaling, and cortactin-cytoskeleton function leading to keratinocyte adhesion and differentiation. *J Biol Chem.* 2004;279(28):29654-69.

31. Calautti E, Grossi M, Mammucari C, Aoyama Y, Pirro M, Ono Y, et al. Fyn tyrosine kinase is a downstream mediator of Rho/PRK2 function in keratinocyte cell-cell adhesion. *J Cell Biol.* 2002;156(1):137-48.

32. Lee SJ, Hwang J, Jeong HJ, Yoo M, Go GY, Lee JR, et al. PKN2 and Cdo interact to activate AKT and promote myoblast differentiation. *Cell Death Dis.* 2016;7(10):e2431.

33. Danno S, Kubouchi K, Mehruba M, Abe M, Natsume R, Sakimura K, et al. PKN2 is essential for mouse embryonic development and proliferation of mouse fibroblasts. *Genes Cells.* 2017;22(2):220-36.

34. Quetier I, Marshall JJT, Spencer-Dene B, Lachmann S, Casamassima A, Franco C, et al. Knockout of the PKN Family of Rho Effector Kinases Reveals a Non-redundant Role for PKN2 in Developmental Mesoderm Expansion. *Cell Rep.* 2016;14(3):440-8.

35. Biondi RM, Cheung PC, Casamayor A, Deak M, Currie RA, and Alessi DR. Identification of a pocket in the PDK1 kinase domain that interacts with PIF and the C-terminal residues of PKA. *EMBO J.* 2000;19(5):979-88.

36. Takasaki J, Saito T, Taniguchi M, Kawasaki T, Moritani Y, Hayashi K, et al. A novel Galphaq/11-selective inhibitor. *J Biol Chem.* 2004;279(46):47438-45.

37. Tzima E, Irani-Tehrani M, Kiosses WB, Dejana E, Schultz DA, Engelhardt B, et al. A mechanosensory complex that mediates the endothelial cell response to fluid shear stress. *Nature.* 2005;437(7057):426-31.

38. Boo YC, Sorescu GP, Bauer PM, Fulton D, Kemp BE, Harrison DG, et al. Endothelial NO synthase phosphorylated at SER635 produces NO without requiring intracellular calcium increase. *Free Radic Biol Med.* 2003;35(7):729-41.

39. Schleicher M, Yu J, Murata T, Derakhshan B, Atochin D, Qian L, et al. The Akt1-eNOS axis illustrates the specificity of kinase-substrate relationships in vivo. *Sci Signal.* 2009;2(82):ra41.

40. Luo Z, Fujio Y, Kureishi Y, Rudic RD, Daumerie G, Fulton D, et al. Acute modulation of endothelial Akt/PKB activity alters nitric oxide-dependent vasomotor activity in vivo. *J Clin Invest.* 2000;106(4):493-9.

41. Mukai Y, Rikitake Y, Shiojima I, Wolfrum S, Satoh M, Takeshita K, et al. Decreased vascular lesion formation in mice with inducible endothelial-specific expression of protein kinase Akt. *J Clin Invest.* 2006;116(2):334-43.

42. Fayard E, Xue G, Parcellier A, Bozulic L, and Hemmings BA. Protein kinase B (PKB/Akt), a key mediator of the PI3K signaling pathway. *Curr Top Microbiol Immunol.* 2010;346:31-56.

43. Go YM, Park H, Maland MC, Darley-Usmar VM, Stoyanov B, Wetzker R, et al. Phosphatidylinositol 3-kinase gamma mediates shear stress-dependent activation of JNK in endothelial cells. *Am J Physiol.* 1998;275(5):H1898-904.

44. Alessi DR, James SR, Downes CP, Holmes AB, Gaffney PR, Reese CB, et al. Characterization of a 3-phosphoinositide-dependent protein kinase which phosphorylates and activates protein kinase Balpha. *Curr Biol.* 1997;7(4):261-9.

45. Alessi DR, Andjelkovic M, Caudwell B, Cron P, Morrice N, Cohen P, et al. Mechanism of activation of protein kinase B by insulin and IGF-1. *EMBO J.* 1996;15(23):6541-51.

46. Sarbassov DD, Guertin DA, Ali SM, and Sabatini DM. Phosphorylation and regulation of Akt/PKB by the rictor-mTOR complex. *Science.* 2005;307(5712):1098-101.

47. Hresko RC, and Mueckler M. mTOR.RICTOR is the Ser473 kinase for Akt/protein kinase B in 3T3-L1 adipocytes. *J Biol Chem.* 2005;280(49):40406-16.

48. Koh H, Lee KH, Kim D, Kim S, Kim JW, and Chung J. Inhibition of Akt and its anti-apoptotic activities by tumor necrosis factor-induced protein kinase C-related kinase 2 (PRK2) cleavage. *J Biol Chem.* 2000;275(44):34451-8.

49. Patel H, Li J, Herrero A, Kroboth J, Byron A, Kriegsheim AV, et al. Novel roles of PRK1 and PRK2 in cilia and cancer biology. *Sci Rep.* 2020;10(1):3902.

50. Tzima E, del Pozo MA, Shattil SJ, Chien S, and Schwartz MA. Activation of integrins in endothelial cells by fluid shear stress mediates Rho-dependent cytoskeletal alignment. *EMBO J.* 2001;20(17):4639-47.

51. Xu S, Ha CH, Wang W, Xu X, Yin M, Jin FQ, et al. PECAM1 regulates flow-mediated Gab1 tyrosine phosphorylation and signaling. *Cell Signal.* 2016;28(3):117-24.

52. Taniyama Y, Weber DS, Rocic P, Hilenski L, Akers ML, Park J, et al. Pyk2- and Src-dependent tyrosine phosphorylation of PDK1 regulates focal adhesions. *Mol Cell Biol.* 2003;23(22):8019-29.

53. Gocher AM, Azabdaftari G, Euscher LM, Dai S, Karacosta LG, Franke TF, et al. Akt activation by Ca(2+)/calmodulin-dependent protein kinase kinase 2 (CaMKK2) in ovarian cancer cells. *J Biol Chem.* 2017;292(34):14188-204.

54. Kashiwagi S, Atochin DN, Li Q, Schleicher M, Pong T, Sessa WC, et al. eNOS phosphorylation on serine 1176 affects insulin sensitivity and adiposity. *Biochem Biophys Res Commun.* 2013;431(2):284-90.

55. Atochin DN, Wang A, Liu VW, Critchlow JD, Dantas AP, Looft-Wilson R, et al. The phosphorylation state of eNOS modulates vascular reactivity and outcome of cerebral ischemia in vivo. *J Clin Invest.* 2007;117(7):1961-7.

56. Li Q, Atochin D, Kashiwagi S, Earle J, Wang A, Mandeville E, et al. Deficient eNOS phosphorylation is a mechanism for diabetic vascular dysfunction contributing to increased stroke size. *Stroke.* 2013;44(11):3183-8.

57. Eroglu E, Saravi SSS, Sorrentino A, Steinhorn B, and Michel T. Discordance between eNOS phosphorylation and activation revealed by multispectral imaging and chemogenetic methods. *Proc Natl Acad Sci U S A.* 2019;116(40):20210-7.

58. Salerno JC, Harris DE, Irizarry K, Patel B, Morales AJ, Smith SM, et al. An autoinhibitory control element defines calcium-regulated isoforms of nitric oxide synthase. *J Biol Chem.* 1997;272(47):29769-77.

59. McCabe TJ, Fulton D, Roman LJ, and Sessa WC. Enhanced electron flux and reduced calmodulin dissociation may explain "calcium-independent" eNOS activation by phosphorylation. *J Biol Chem.* 2000;275(9):6123-8.

60. Lane P, and Gross SS. Disabling a C-terminal autoinhibitory control element in endothelial nitric-oxide synthase by phosphorylation provides a molecular explanation for activation of vascular NO synthesis by diverse physiological stimuli. *J Biol Chem.* 2002;277(21):19087-94.

61. Powell DW, Rane MJ, Chen Q, Singh S, and McLeish KR. Identification of 14-3-3zeta as a protein kinase B/Akt substrate. *J Biol Chem.* 2002;277(24):21639-42.

62. Korhonen H, Fisslthaler B, Moers A, Wirth A, Habermehl D, Wieland T, et al. Anaphylactic shock depends on endothelial Gq/G11. *J Exp Med.* 2009;206(2):411-20.

63. Sorensen I, Adams RH, and Gossler A. DLL1-mediated Notch activation regulates endothelial identity in mouse fetal arteries. *Blood.* 2009;113(22):5680-8.

64. Farley FW, Soriano P, Steffen LS, and Dymecki SM. Widespread recombinase expression using FLPeR (flipper) mice. *Genesis.* 2000;28(3-4):106-10.

65. Ishii K, Sheng H, Warner TD, Forstermann U, and Murad F. A simple and sensitive bioassay method for detection of EDRF with RFL-6 rat lung fibroblasts. *Am J Physiol.* 1991;261(2 Pt 2):H598-603.

66. Bailey RJ, Walker CS, Ferner AH, Loomes KM, Prijic G, Halim A, et al. Pharmacological characterization of rat amylin receptors: implications for the identification of amylin receptor subtypes. *Br J Pharmacol.* 2012;166(1):151-67.

67. Liu C, Ngai CY, Huang Y, Ko WH, Wu M, He GW, et al. Depletion of intracellular Ca2+ stores enhances flow-induced vascular dilatation in rat small mesenteric artery. *Br J Pharmacol.* 2006;147(5):506-15.

68. Kim HT, Yin W, Jin YJ, Panza P, Gunawan F, Grohmann B, et al. Myh10 deficiency leads to defective extracellular matrix remodeling and pulmonary disease. *Nat Commun.* 2018;9(1):4600.

69. Kiweler M, Looso M, and Graumann J. MARMoSET - Extracting Publication-ready Mass Spectrometry Metadata from RAW Files. *Mol Cell Proteomics.* 2019;18(8):1700-2.

70. Cox J, and Mann M. MaxQuant enables high peptide identification rates, individualized p.p.b.-range mass accuracies and proteome-wide protein quantification. *Nat Biotechnol.* 2008;26(12):1367-72.

71. Cox J, Neuhauser N, Michalski A, Scheltema RA, Olsen JV, and Mann M. Andromeda: a peptide search engine integrated into the MaxQuant environment. *J Proteome Res.* 2011;10(4):1794-805.

72. UniProt C. UniProt: a worldwide hub of protein knowledge. *Nucleic Acids Res.* 2019;47(D1):D506-D15.

Figures and Figure legends

Figure 1

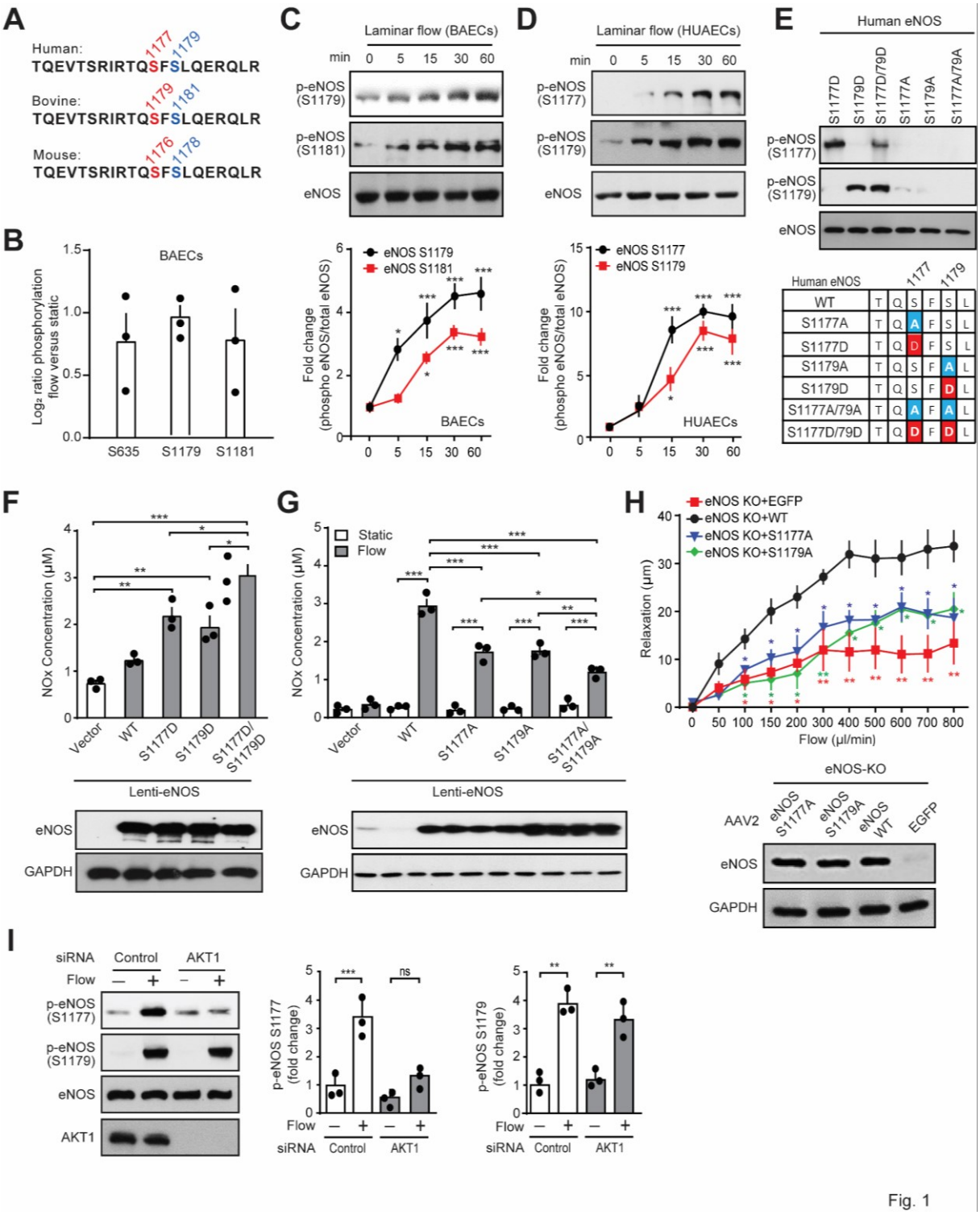

Figure 1.

Figure 1. Flow induces eNOS phosphorylation at serine 1177 and 1179. (**A**) eNOS amino acid sequence of different species. (**B**) Phosphorylation of eNOS serine residues of BAECs exposed to laminar flow (15 dynes/cm^2) determined by LC-MS/MS.

Shown are the fold changes of the corrected ratios of flow versus static conditions (n=3). (**C**,**D**) BAECs (C) or HUAECs (D) were exposed to laminar flow (15 dynes/cm^2). and total and phosphorylated eNOS was determined by immunoblotting. Graphs show the densitometric evaluation (n=3 independent experiments). (**E**) HEK293 cells expressing the indicated mutants of human eNOS were lyzed and analyzed by immunoblotting using phosphosite-specific. (**F**,**G**) Wild-type (WT) or mutated human eNOS were expressed by lentiviral transduction after siRNA mediated eNOS knockdown in HUAECs, and the nitrate/nitrite concentration in the cell culture medium was determined in the absence (F) or depending on flow (G). Expression of eNOS was analyzed by immunoblotting (F,G, lower panels) (n=3 independent experiments). (**H**) eNOS$^{-/-}$ mice were infected with AAV2-QuadYF virus transducing wild-type or mutant eNOS or EGFP. 7 days later, carotid arteries were isolated and flow-induced vasorelaxation was analyzed. The immunoblot demonstrates equal expression levels of different eNOS mutants. (**I**) HUAECs transfected with control siRNA or siRNAs directed against AKT1 were exposed to laminar flow (15 dynes/cm^2). Total AKT and total and phosphorylated eNOS were determined by immunoblotting. Bar diagrams show the densitometric evaluation of blots (n=3 independent experiments). Data represent the mean ± SEM; *, $p \leq 0.05$; **, $p \leq 0.01$; ***, $p \leq 0.001$ (two-way ANOVA with Bonferroni's post-hoc test (C, D, G, H; P-values in H describe difference compared to eNOS-WT), one-way ANOVA, with Tukey's post-hoc test (F and I)). P-values in 1c and d describe difference compared to time point zero.

Figure 2

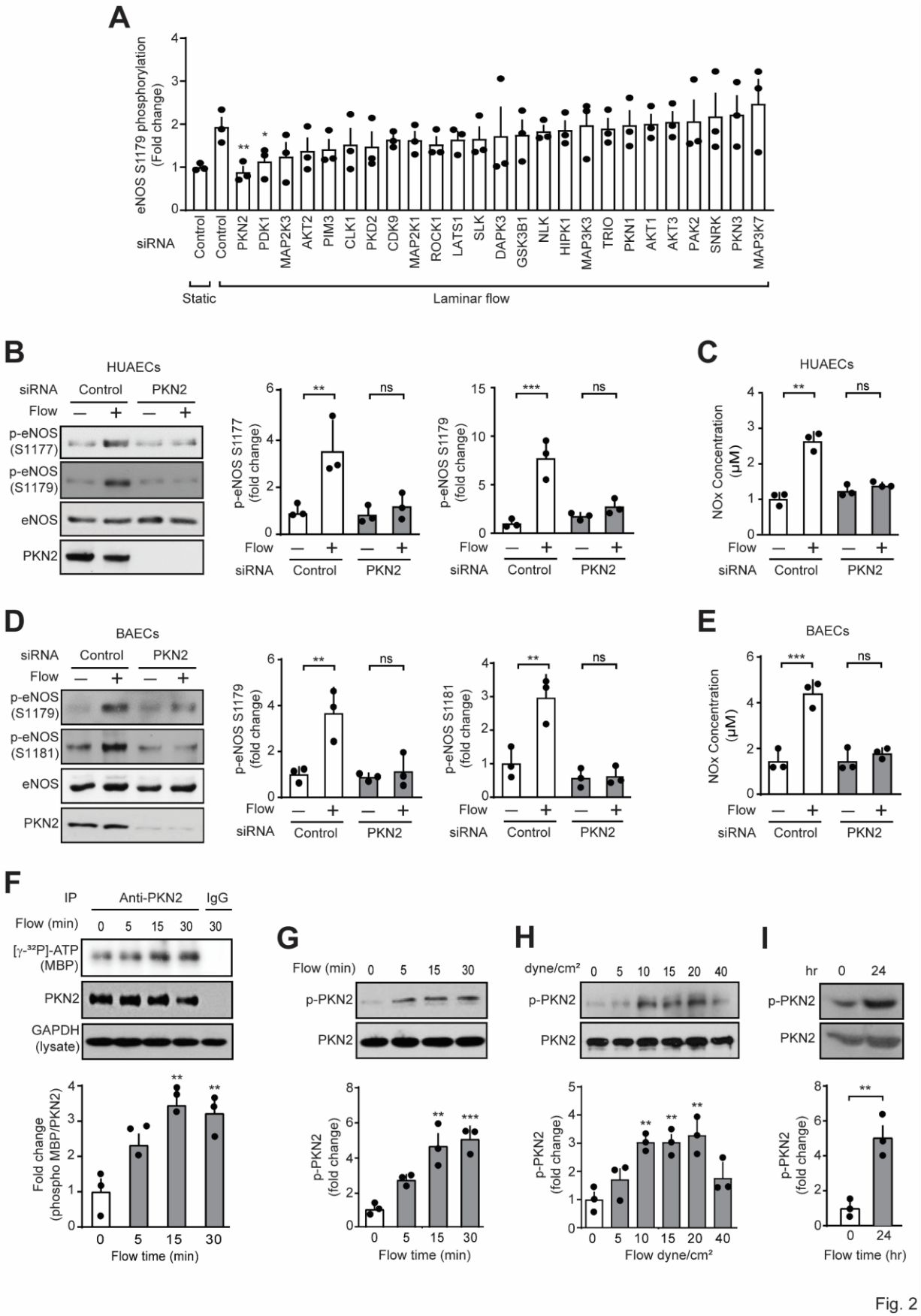

Fig. 2

Figure 2. PKN2 is activated by flow and mediates phosphorylation of eNOS at serine 1177 and 1179. (**A**) HUAECs were transfected with control siRNA or siRNAs directed against the indicated protein kinases and were kept under static conditions

(static) or were exposed to laminar flow (15 dynes/cm^2) for 15 min. Shown is the ratio of flow-induced phosphorylation of eNOS at serine 1179 in cells transfected with control siRNA and an siRNA against a particular protein kinase. The plot shows the ranked average ratios of 3 independent experiments. (**B**-**E**) HUAECs (B,C) or BAECs (D, E) were transfected with control or siRNA against PKN2 and were exposed to laminar flow (15 dynes/cm^2). Total and phosphorylated eNOS as well as PKN2 were determined by immunoblotting (B,D), or nitrate/nitrite levels were determined in the supernatants (C,E). Bar diagrams show the densitometric evaluation of blots (n=3 independent experiments). (**F**-**I**) HUAECs were exposed to laminar flow (15 dynes/cm^2, if not stated otherwise) for the indicated time periods. Thereafter, PKN2 was immunoprecipitated and its kinase activity was determined as described in the Methods section (F), or total as well as phosphorylated PKN2 was determined by immunoblotting (G-I). Bar diagrams show the densitometric evaluation of blots (n=3 independent experiments). Data represent the mean ± SEM; *P ≤ 0.05, **P ≤ 0.01, ***P ≤ 0.001, (two-way ANOVA with Bonferroni's post-hoc test (A), one-way ANOVA, with Tukey's post-hoc test (B-H), unpaired two-tailed Student's t-test (I)).

Figure 3

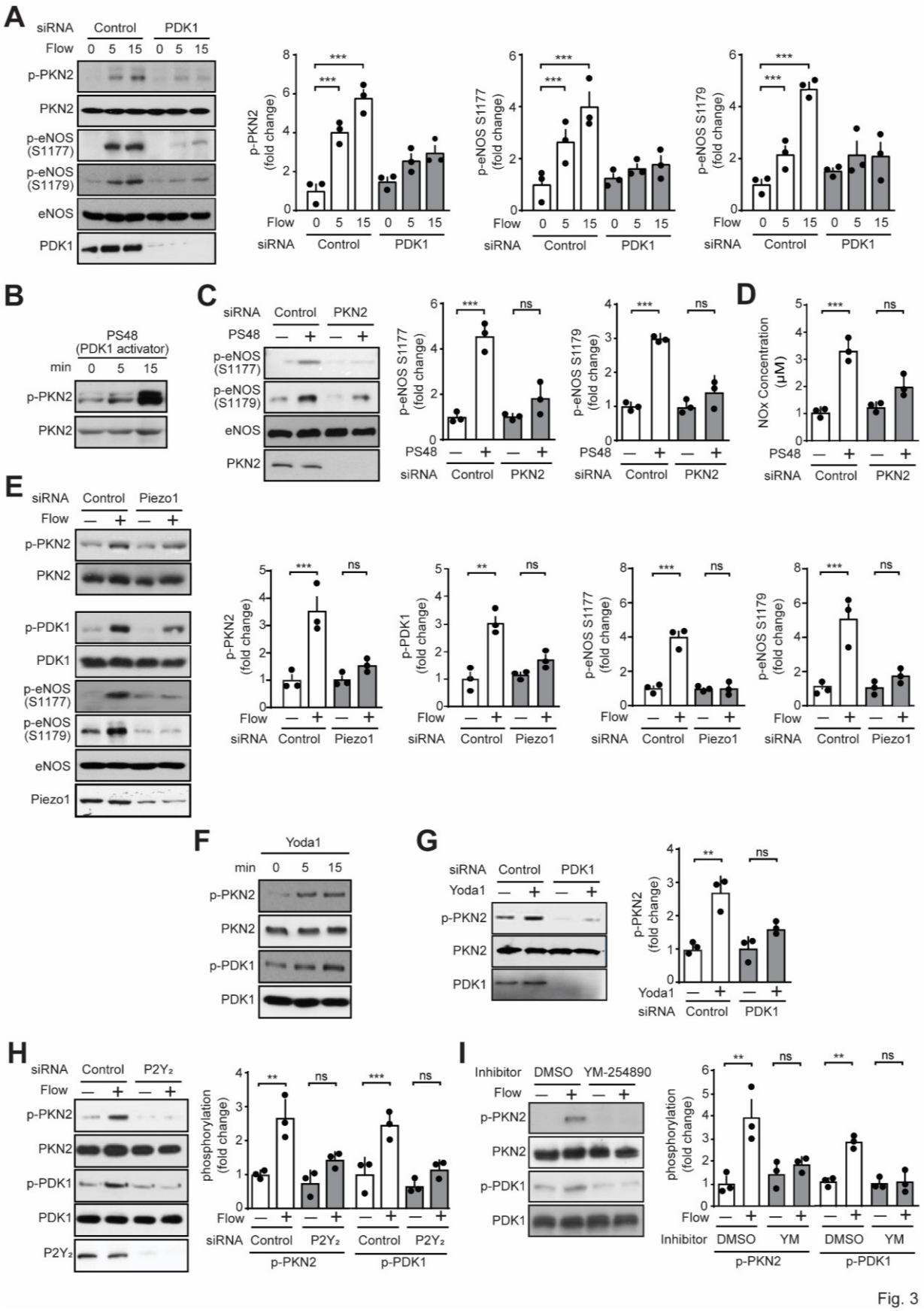

Fig. 3

Figure 3. Flow-induced PKN2 activation involves Piezo1, G_q/G_{11} and PDK1. (**A-I**) HUAECs were transfected with control siRNA or siRNAs directed against PDK1 (A,G), PKN2 (C,D), Piezo1 (E), $P2Y_2$ (H) or were left untransfected (B,F) or were pretreated without or with 100 nM of YM-254890 (YM) (I) for 30 min. Thereafter, cells were exposed to laminar flow (15 dynes/cm^2) for 15 min or the indicated time periods (A,E,H,I) or to 5 µM of PS48 for 15 min or the indicated time periods (B-D) or to 1 µM of Yoda1 for 15 min or the indicated time periods (F,G). Phosphorylation or total amount of the indicated proteins was determined in lysates by immunoblotting (A-C, E-I), or the concentration of nitrate/nitrite was measured in the supernatant (D). Bar diagrams in A,C,F-I show the densitometric analysis of blots (n=3 independent experiments). Data represent mean ± SEM; *, $P \leq 0.05$; **, $P \leq 0.01$ ***, $P \leq 0.001$ (one-way ANOVA with Tukey's post-hoc test).

Figure 4

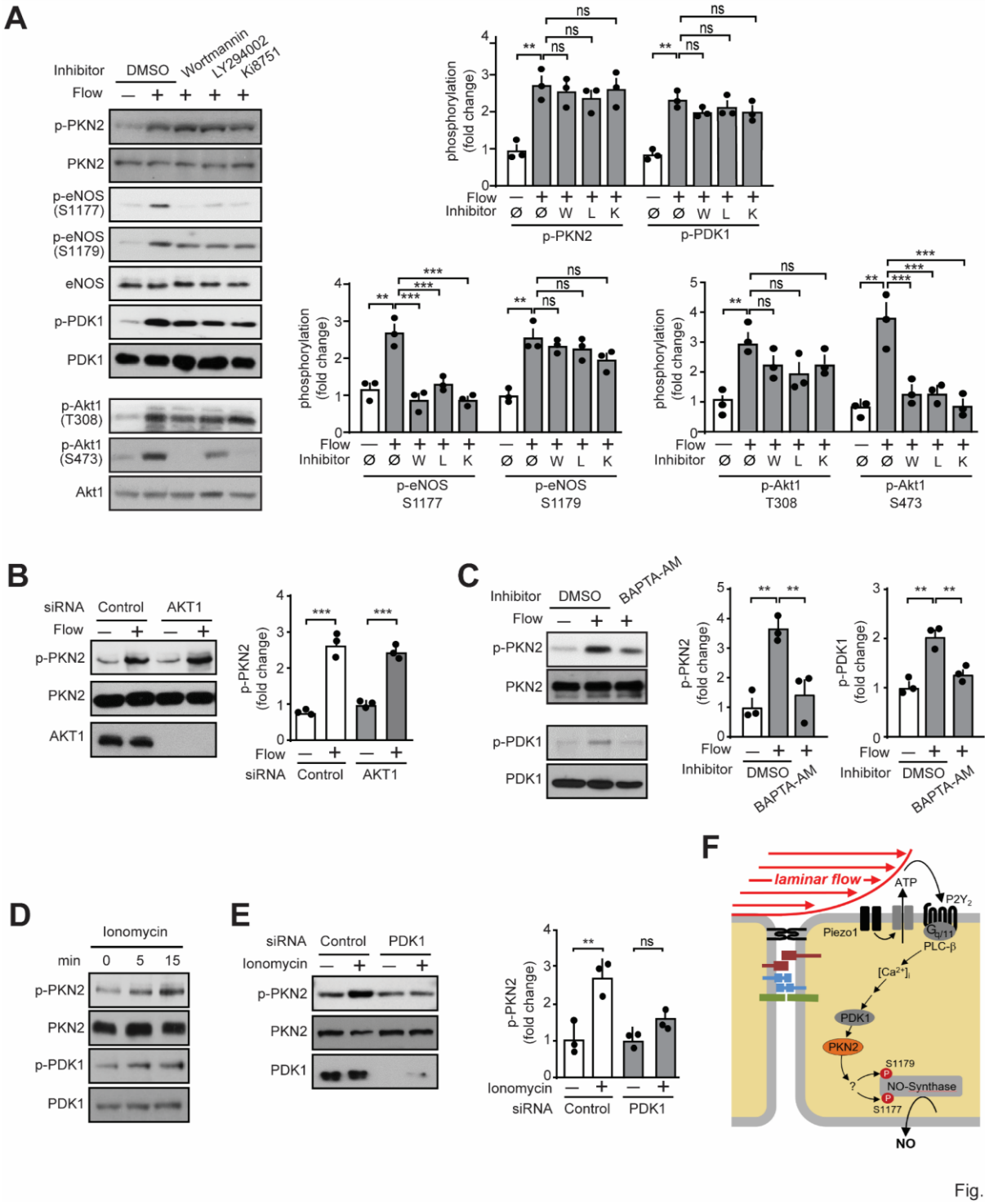

Fig.

Figure 4. Flow-induced PKN2 activation involves Ca^{2+} but not PI-3-kinase and AKT. (**A-E**) HUAECs were preincubated for 30 minutes with PI3K inhibitors wortmannin (100 nM), LY294002 (10 µM) or the VEGFR2 inhibitor Ki8751 (500 nM) (A) or with 20 µM of BAPTA-AM (C) or were transfected with control siRNA or siRNAs directed against AKT1 (B) or PDK1 (E) or were without pretreatment (D). Thereafter, cells were exposed to flow (15 dynes/cm^2) for 15 min (A-C) or to 1 µM of ionomycin (D,E) for 15 min or the indicated time periods. Phosphorylation and total amount of the indicated proteins was determined in lysates by immunoblotting. Bar diagrams show

the densitometric analysis of blots (n=3 independent experiments). The control immunoblot for AKT1 in B is from the same experiment as the one shown in Fig. 1I. (**F**) Model of the mechanism mediating laminar flow-induced PKN2 activation resulting in eNOS phosphorylation and activation. Data represent mean ± SEM; *, P ≤ 0.05; **, P ≤ 0.01 ***, P ≤ 0.001 (one-way ANOVA, with Tukey's post-hoc test).

Figure 5

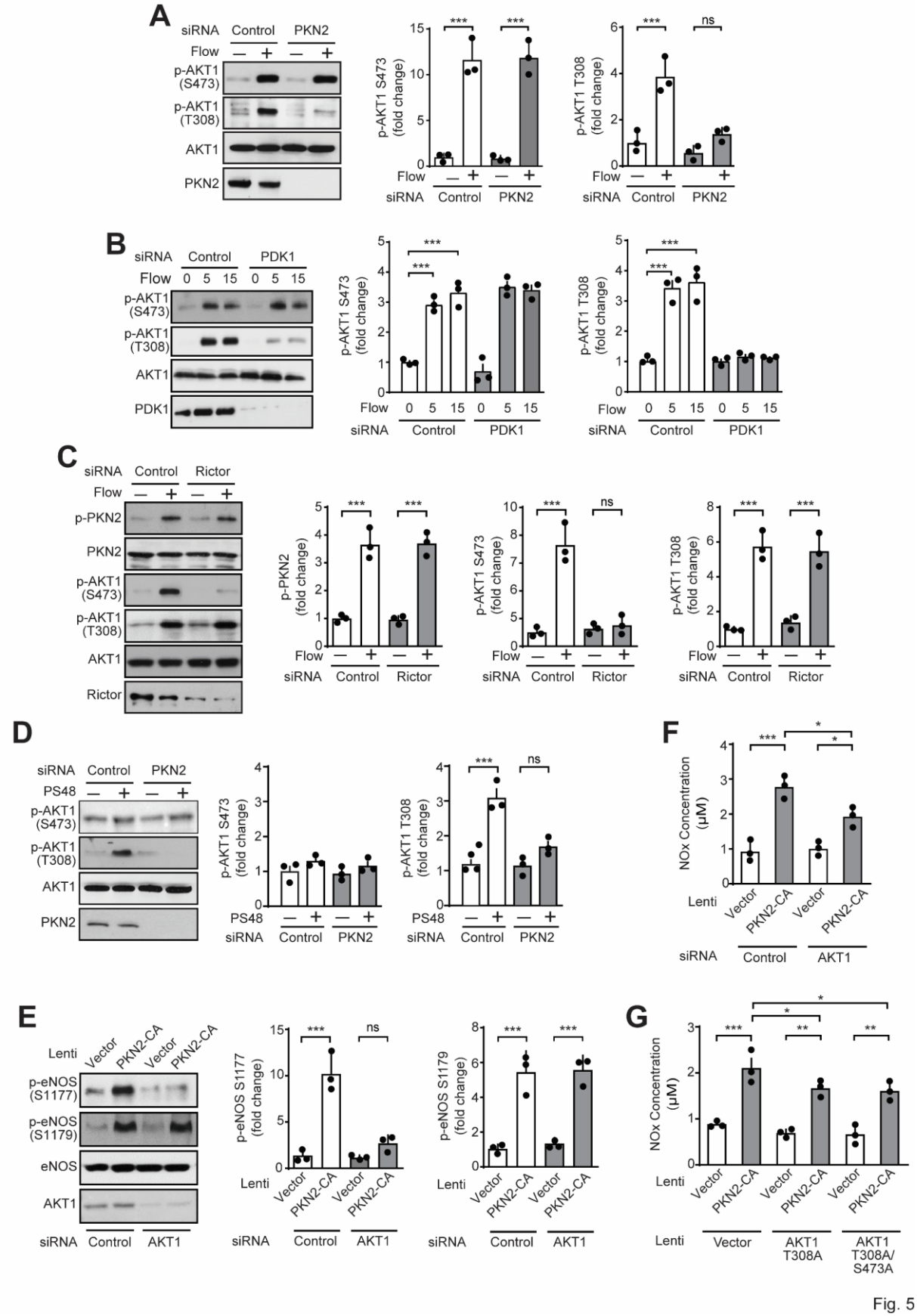

Figure 5. PKN2 mediates phosphorylation of AKT at threonine 308 but not at serine 473. (**A-G**) HUAECs were transfected with control siRNA or siRNAs directed against PKN2 (A,D-G), PDK1 (B), Rictor (C) or AKT1 (E-G) and were then exposed to

laminar flow (15 dynes/cm^2) for 15 min or the indicated time periods (A-C) or to 5 µM of PS48 for 15 min (D). Alternatively, a constitutively active mutant of PKN2 (PKN-CA) (E-G) as well as the indicated phosphosite mutants of AKT1 (G) were expressed by lentiviral transduction after siRNA-mediated knockdown of AKT1 (E,F) in HUAECs. Phosphorylation or total amount of the indicated proteins was determined in lysates by immunoblotting (A-E), or the concentration of nitrate/nitrite was measured in the supernatant (F,G). Bar diagrams in a-e show the densitometric evaluation of blots (n=3 independent experiments). Control immunoblots for PKN2 and PDK1 knock-down efficiency in A, B and D are from the same experiments as those shown in Figs. 2B, 3A and 3C, respectively. Data represent mean ± SEM; *, P ≤ 0.05; **, P ≤ 0.01 ***, P ≤ 0.001 (one-way ANOVA, with Tukey's post-hoc test (A-F), two-way ANOVA with Bonferroni's post-hoc test (G)).

Figure 6

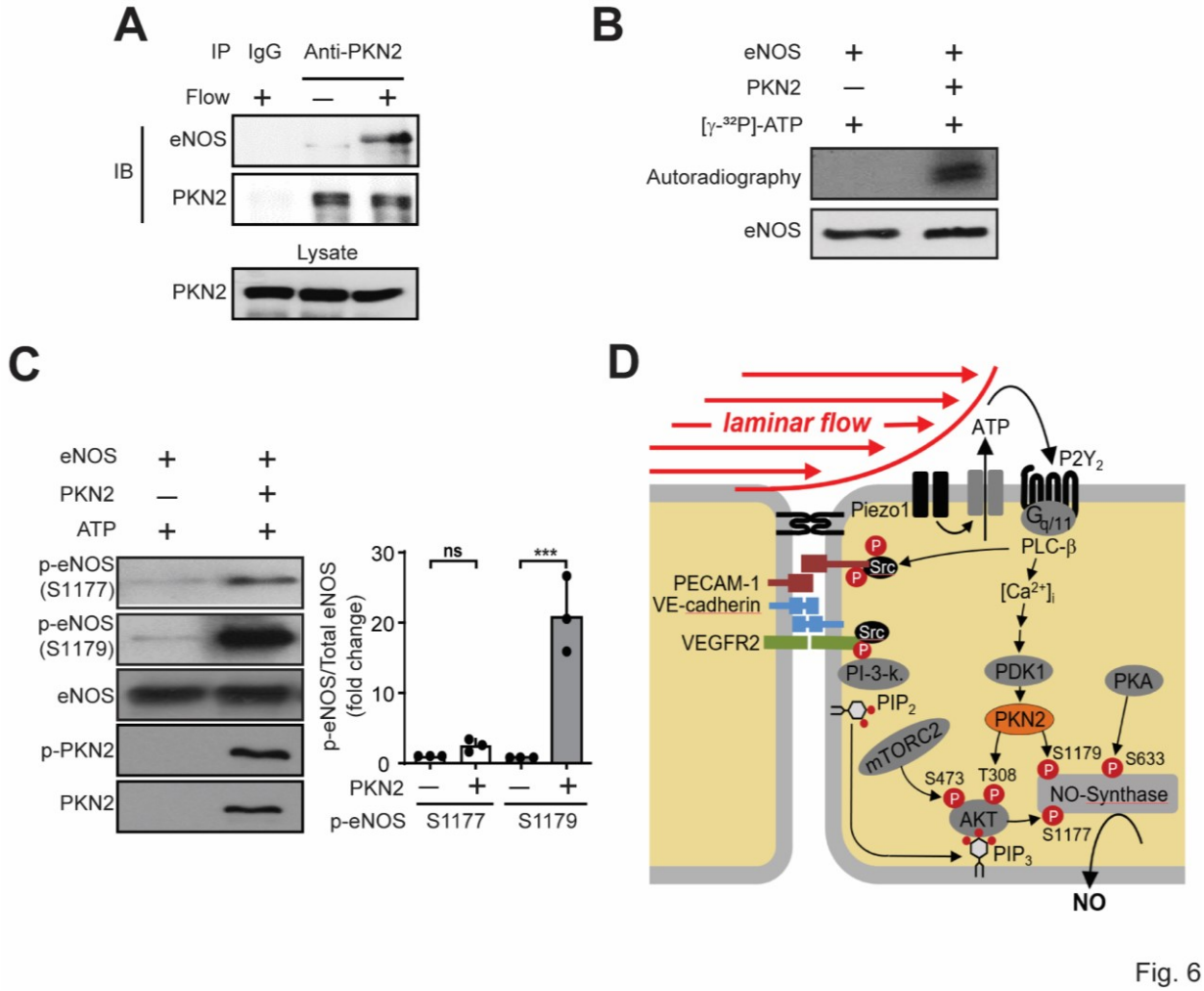

Fig. 6

Figure 6. PKN2 mediates eNOS activation by direct phosphorylation of serine 1179 and by AKT-dependent phosphorylation of serine 1177. (**A**) HUAECs kept untreated or exposed to flow were lyzed, and PKN2 was immunoprecipitated with a specific antibody. IgG served as a negative control. Shown are immunoblots of the lysate and the immunoprecipitate using anti-eNOS and anti-PKN2 antibodies. (**B**, **C**) Purified eNOS was incubated in kinase buffer without or with recombinant purified PKN2 together with 50 µM [γ-^{32}P]-ATP (3000 Ci/mmol/L) (B) or ATP (C) for 30 minutes at 30°C. Thereafter samples were separated by SDS-PAGE. Shown are an autoradiogram and a Coomassie stain of the gel (B). Alternatively, an immunoblotting analysis was performed using antibodies recognizing eNOS and PKN2 protein or the eNOS S1177 and S1179 as well as PKN2 T816 phosphosites (C). (**D**) Model of the role of PKN2 in flow-induced phosphorylation of eNOS.

Figure 7

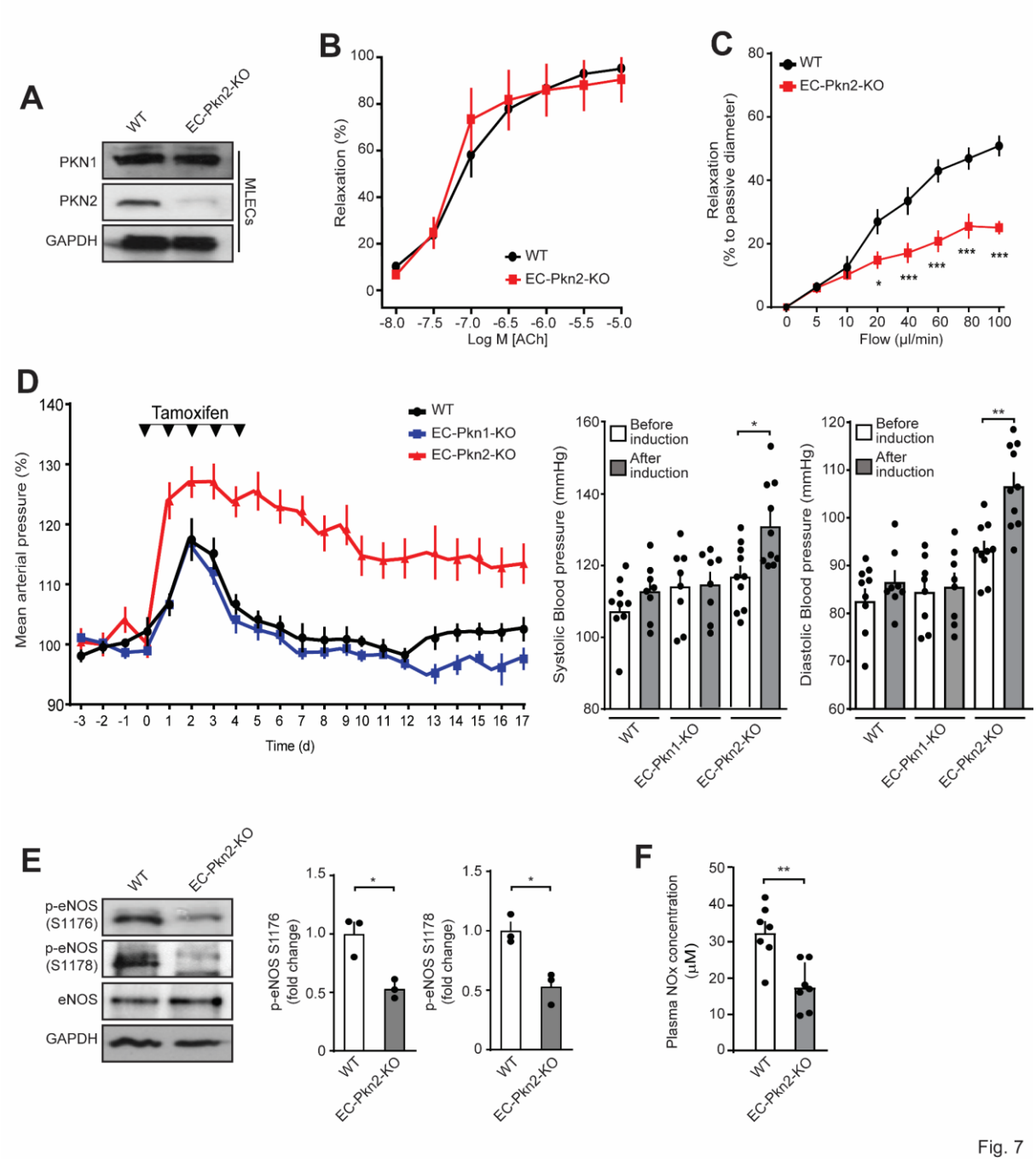

Fig. 7

Figure 7. Endothelial PKN2 deficiency results in loss of flow-induced vasodilation and arterial hypertension. (**A**) Immunoblotting analysis of PKN1 and PKN2 expression in mouse lung endothelial cells (MLEC) from 8-week-old wild-type (WT) and induced EC-Pkn2-KO mice. (**B**) Effect of acetylcholine on the tone of mesenteric artery stripes from wild-type (WT) (n=7) and EC-Pkn2-KO animals (n=7) were determined after precontraction with 10 µM phenylephrine. (**C**) Mesenteric arteries isolated from tamoxifen-treated WT or EC-Pkn2-KO mice were precontracted with 100 nM of the thromboxane A_2 analog U46619 and were then exposed to stepwise increases in perfusion flow. Flow-induced vasorelaxation is shown as percentage of

the passive vessel diameter (n=7 mice, WT and EC-Pkn2-KO). (**D**) Blood pressure in WT (n=12), EC-Pkn1-KO mice (n=8) and EC-Pkn2-KO (n=12) animals before, during and after induction of tamoxifen. Average blood pressure 3 days before induction was set to 100 %. The bar diagram shows systolic and diastolic arterial blood pressure 4 days before tamoxifen treatment and in the second week after induction. (**E**) eNOS phosphorylation at S1176 and 1178 in lysates from mesenteric arteries prepared from tamoxifen-treated WT and EC-Pkn2-KO mice (n=3 animals). (**F**) Plasma nitrate and nitrite (NOx) levels in WT (n=7) and EC-Pkn2-KO mice (n=7) 10 days after induction. Data represent the mean ± SEM; *P ≤ 0.05, **P ≤ 0.01, ***P ≤ 0.001, (two-way ANOVA with Bonferroni's post-hoc test (B and C), paired two-tailed Student's t-test (D) or unpaired two-tailed Student's t-test (F)).